New combination of four-component gas He–Ne–Xe–Ar for high efficiency plasma display panel

Byoung-Kuk Min, Hoon-Young Choi, Seok-Hyun Lee, and Heung-Sik Tae[a)]
School of Electrical and Computer Engineering, Inha University, Inchon, Korea

(Received 16 February 2000; accepted 23 October 2000)

The improvement of luminous efficiency is one of the most important issues in making a plasma display into a large flat panel device. Accordingly, a new combination of a four-component gas, He–Ne–Xe–Ar, is proposed in order to achieve a high luminous efficiency in color plasma display panels (PDP). The densities of 32 species and electron temperature were calculated using a zero-dimensional simulation. The results were then compared with measurements of brightness and luminous efficiency to identify the optimum mixing condition of He(7): Ne(3)–Xe(4%)–Ar gas for a color PDP. The reaction mechanism was computationally analyzed to comprehend the discharge mechanism in He–Ne–Xe–Ar as well as in He–Ne–Xe. By simulation, the maximum peak point of the Xe*($^1S_4$) state was obtained between a 0.1% and 0.5% Ar mixing ratio and the maximum luminous efficiency was measured with a 0.3% Ar mixing ratio in the PDP. As a result, the luminous efficiency was considerably improved (about 20%) with a 0.3% Ar addition, compared with the conventional He–Ne–4% Xe mixing gas. © *2001 American Vacuum Society.*
[DOI: 10.1116/1.1333077]

I. INTRODUCTION

A surface discharge ac plasma display panel (PDP) offers good characteristics such as a simple structure, high resolution, fast response, and wide viewing angle. However, the luminance and luminous efficiency are both unsatisfactory for use in a TV set or multimedia monitor, compared with cathode ray tubes (CRTs). Accordingly, the improvement of the luminance and luminous efficiency in color plasma display panels is a crucial area for development and there have already been many attempts, for example, an addressing scheme, cell structure, pressure, mixing ratio of the rare gas, and phosphor, etc. The enclosed gas directly affects the luminance and luminous efficiency, color purity, lifetime, operating voltage, etc. Many studies about a rare gas mixture have been performed in many countries in order to find out more suitable gas for PDP. For example, there are He–Xe,[1] Ne–Xe,[2] Ne–Kr–Xe,[3] He–Ne–Xe,[4] and Ne–Ar–Xe.[5] Among these gas mixtures, the conventional enclosed gas is He–Ne–Xe. This combination was originally introduced to improve drawbacks such as the high driving voltage and short life-time of a He–Xe gas mixture, and the poor color purity of a Ne–Xe gas mixture. This study proposes an improved luminance and luminous efficiency through the addition of a small amount of Ar gas into the conventional He–Ne–Xe gas.

II. SIMULATION MODEL AND EXPERIMENTS

A numerical zero-dimensional simulation method using chemical reactions with 32 species (He, Xe, Ne, Ar, electron, He^+, He_2^+, He*, He**, He_2^+, Xe*, Xe**, Xe_2^{*1}, Xe_2^{*3}, Xe_2^{**}, Xe^+, Xe_2^+, Xe_3^+, Ne*, Ne**, Ne_2^*, Ne^+, Ne_2^+, Ar*, Ar**, Ar^+, Ar_2^*, Ar_2^{**}, Ar_2^+, $NeXe^+$, ArXe*, $ArXe^+$) and an electron energy equation was used to identify the optimum mixing condition of the He–Ne–Xe–Ar gas in a color plasma display panel.[6,7] The electron temperature and densities of the 32 species were calculated as a function of an Ar mixing ratio ranging from 0% to 10%, particularly, the density of the first excited xenon state, Xe*($^1S_4$), because the Xe* state is directly related with the luminous efficiency. The theories for the governing equations and reaction coefficients have already been published in a previous paper by the current authors.[6] In order to investigate the improvement in the luminous efficiency when Ar gas was added, the same simulation model was used in analyzing the mechanism that Xe* particle and electron are produced and are reduced.

Figure 1 shows a schematic diagram of the luminance measurement system. The experimental apparatus was com-

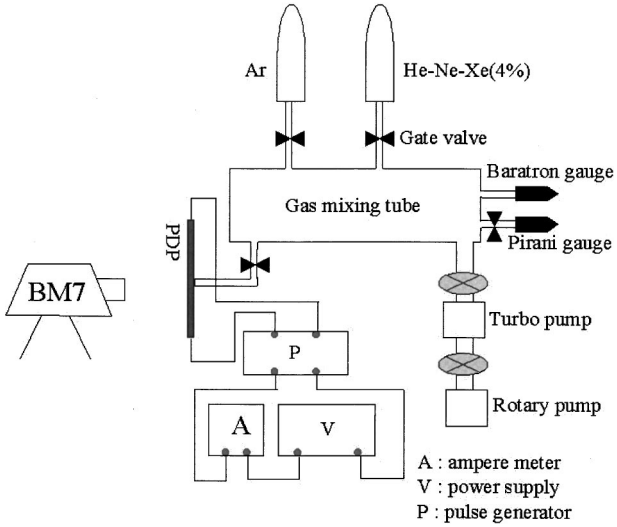

FIG. 1. Schematic diagram of luminance measurement system.

[a)]Present address: School of Electronics and Electrical Engineering, Kyungpook National University, Taegue, Korea.

TABLE I. Specifications of 7.5 in. diagonal test panel.

Panel structure	Direct viewing style
Display area	151×74 mm
Color cell arrangement	Parallel stripe
Tricolor pitch	1.26 mm
Phosphor R	$Y,Gd(BO_3):Eu^{3+}$
G	$ZnSiO_4:Mn^{2+}$
B	$BaMgAl_{10}O_{17}:Eu^{2+}$
Effective sustain freq.	5 KHz

posed of a 7.5 in. (diagonal size) plasma display panel with RGB phosphor, a gas distributor, pump system, and driving circuit. The 7.5 in. diagonal test panel consists of two glasses. On the upper glass substrate, the parallel electrode array with 70 μm gap is formed. Discharge occurs between each pair of electrodes. A dielectric layer is printed on the electrodes, and MgO protection layer is deposited over the entire discharge surface. On the other glass substrate, data electrode, barrier rib, and phosphor are formed. The test panel specifications are summarized in Table I. The base pressure of the gas distributor and panel was lower than 10^{-6} Torr. The Ar gas and the premixed He–Ne–Xe(4%) were mixed in a mixing tube. The ratio of He to Ne was 7:3 and the Xe concentration in the He–Ne–Xe gas was 4%. A panel was mounted at the end of the mixing tube. The gas discharge was maintained by a driving circuit system which can control pulse duration time and voltage. The driving voltage frequency is 5 kHz. The brightness was measured by a BM7 (Topcon, Japan) and the displacement current and discharge current were measured using a multimeter TX3 (Tektronix, USA).

III. RESULTS AND DISCUSSION

Figure 2 shows the electron temperature as a function of the Ar mixing ratio. The electron temperature decreases as the Ar mixing ratio increases. The main reason for this is that

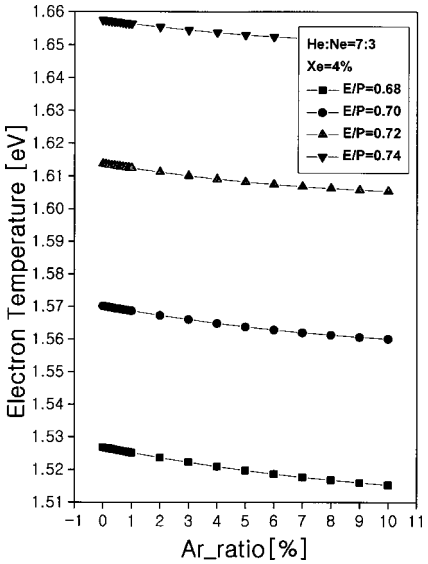

FIG. 2. Electron temperatures (He:Ne=7:3, Xe=4%, P=400 Torr).

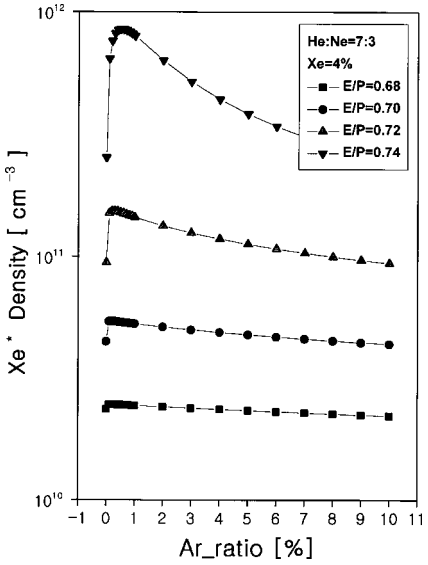

FIG. 3. Xe* densities as a function of Ar concentration (He:Ne=7:3, Xe=4%, P=400 Torr).

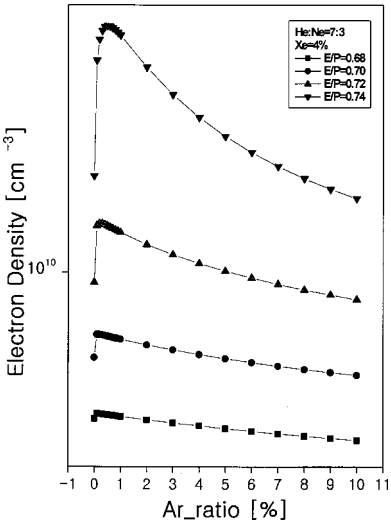

FIG. 4. Electron densities as a function of Ar concentration (He:Ne=7:3, Xe=4%, P=400 Torr).

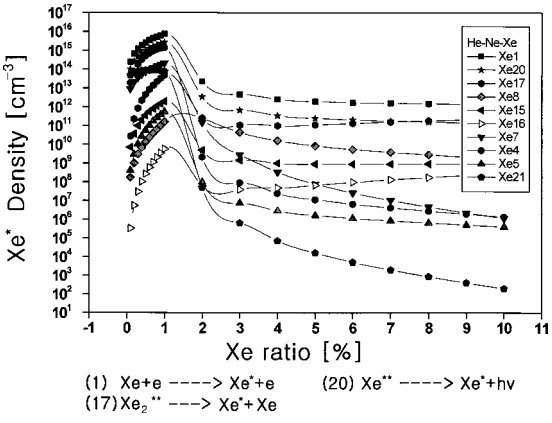

FIG. 5. Xe* densities produced as a result of each reaction equation in a Ne–Xe–He gas mixture (P=400 Torr).

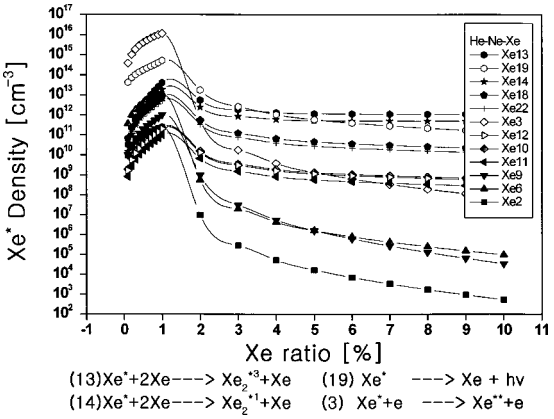

FIG. 6. Xe* densities reduced as a result of each reaction equation in a Ne–Xe–He gas mixture ($P=400$ Torr).

the mean free path of an electron in the mixed gas decreases as the amount of Ar gas increases due to the large electron collision cross section of Ar.

Figure 3 shows the density of the Xe* species as a function of Ar gas mixing ratios from 0.1% to 10%. According to the various E/P[V/cm Torr] values, the density of the Xe* species increases with Ar gas mixing ratios between 0.1% and 0.5% when compared with the three-component gas He–Ne–4% Xe. From these results, it can be predicted that the luminance of the four-component gas He–Ne–Xe–Ar with Ar gas mixing ratio of around 0.5% will be higher than that of the three-component gas He–Ne–Xe.

Figure 4 shows the density of electron as a function of Ar gas mixing ratios from 0.1% to 10%. The trend of electron density is very similar to that of Xe* density. From these results, it can be predicted that the operating voltage of the

TABLE II. Reaction equations related to Xe* in He–Ne–Xe–Ar gas mixture.

No.	Reaction equation	Rate coefficient	Reference
1	$Xe+e\rightarrow Xe^*+e$	$1.2\times10^{-8}\times T_e^{-0.72}\times e^{(-8.32/T_e)}$	8
2	$Xe^*+e\rightarrow Xe+e$	3.0×10^{-9}	8
3	$Xe^*+e\rightarrow Xe^{**}+e$	3.0×10^{-7}	8
4	$Xe^{**}+e\rightarrow Xe^*+e$	8.0×10^{-7}	8
5	$Xe_2^*+e\rightarrow Xe^*+Xe+e$	2.0×10^{-7}	8
6	$Xe^*+e\rightarrow Xe^++2e$	2.7×10^{-9}	8
7	$Xe_2^++e\rightarrow Xe^*+Xe$	$1.4\times10^{-6}\times(T_e/300\text{ K})^{-0.5}$	9
8	$Xe_3^++e\rightarrow Xe^*+2Xe$	9.0×10^{-5}	18
9	$Xe^*+Xe^*\rightarrow Xe^++Xe+e$	8.0×10^{-11}	8
10	$Xe^*+Xe\rightarrow 2Xe$	3.5×10^{-15}	10
11	$Xe^*+Xe\rightarrow Xe^{**}+Xe$	1.5×10^{-15}	13
12	$Xe^*+2Xe\rightarrow Xe_2^*+Xe$	3.0×10^{-15}	13
13	$Xe^*+2Xe\rightarrow Xe_2^{*3}+Xe$	4.4×10^{-32}	8
14	$Xe^*+2Xe\rightarrow Xe_2^{*1}+Xe$	2.0×10^{-32}	8
15	$Xe^{**}+Xe\rightarrow Xe^*+Xe$	2.8×10^{-13}	16
16	$Xe_2^{**}+Xe\rightarrow Xe^*+2Xe$	$1.0\times10^{-11}\times(T_g/300)^{1/2}$	8
17	$Xe_2^{**}\rightarrow Xe^*+Xe$	1.0×10^{8}	8
18	$Xe^*+Xe+He\rightarrow Xe_2^*+He$	1.4×10^{-32}	13
19	$Xe^*\rightarrow Xe+h\upsilon$	1.0×10^{4}	17
20	$Xe^{**}\rightarrow Xe^*+h\upsilon$	1.0×10^{7}	8
21	$NeXe^++e\rightarrow Xe^*+Ne$	$2.0\times10^{-7}\times T_e^{-0.5}$	11
22	$Xe^*+Xe+Ne\rightarrow Xe_2^*+Ne$	2.0×10^{-32}	12
23	$Xe^*+2Ar\rightarrow ArXe^*+Ar$	6.7×10^{-34}	18
24	$Xe^*+Xe+Ar\rightarrow Xe_2^*+Ar$	2.8×10^{-32}	10
25	$Xe^{**}+Ar\rightarrow Xe^*+Ar$	1.0×10^{-10}	18
26	$Ar^*+Xe\rightarrow Xe^*+Ar$	2.2×10^{-10}	18
27	$Ar_2^*+Xe\rightarrow Xe^*+2Ar$	4.4×10^{-10}	19
29	$Xe^*+2Ar\rightarrow ArXe^*+Ar$	6.7×10^{-34}	18
30	$Ar_2^*+Xe\rightarrow 2Ar+Xe^*$	2.4×10^{-10}	10
32	$ArXe^++e\rightarrow Ar+Xe^*$	1.0×10^{-6}	18

TABLE III. Reaction equations related to electron in He–Ne–Xe–Ar gas mixture.

No.	Reaction equation	Reaction coefficient	Reference
11	$Xe+e\rightarrow Xe^++2e$	1.3×10^{-12}	12
12	$Xe^*+e\rightarrow Xe^++2e$	2.7×10^{-9}	8
13	$Xe^{**}+e\rightarrow Xe^++2e$	2.0×10^{-8}	8
14	$Xe_2^*+e\rightarrow Xe_2^++2e$	5.0×10^{-9}	8
15	$Xe_2^{**}+e\rightarrow Xe_2^++2e$	6.0×10^{-18}	8
16	$He+e\rightarrow He^++2e$	$1.5\times10^{-9}\times T_e^{0.68}\times e^{(-24.6/T_e)}$	22
18	$He^*+e\rightarrow He^++2e$	$1.28\times10^{-7}\times T_e^{0.6}\times e^{(-4.87/T_e)}$	22
19	$Xe^++2e\rightarrow Xe^{**}+e$	$5.1\times10^{-27}/T_e^{4.5}$	17
20	$Xe^++e\rightarrow Xe+h\upsilon$	6.4×10^{-7}	17
21	$Xe_2^++e\rightarrow Xe^{**}+Xe$	$2.3\times10^{-7}\times T_e^{-0.7}$	12
22	$Xe_2+e\rightarrow Xe^*+Xe$	$1.4\times10^{-6}\times(T_e/300\text{ K})^{-0.5}$	9
23	$Xe_2^++e\rightarrow 2Xe$	1.4×10^{-6}	13
24	$Xe_3^++e\rightarrow Xe^{**}+2Xe$	$1.0\times10^{-5}\times T_e^{-0.5}$	8
25	$Xe_3^++e\rightarrow Xe^*+2Xe$	9.0×10^{-5}	8
26	$He^++e\rightarrow He$	2.0×10^{-15}	11
27	$He^++2e\rightarrow He^{**}+e$	$5.1\times10^{-27}\times T_e^{-4.5}$	11
28	$He_2^++e\rightarrow 2He$	4.0×10^{-9}	11
29	$He_2^++e\rightarrow He^*+He$	$5.0\times10^{-9}\times T_e^{-0.5}$	22
30	$He_2^++2e\rightarrow He^*+He+e$	4.0×10^{-20}	15
31	$He_2^++e+He\rightarrow He^*+eHe$	5.0×10^{-27}	15
32	$Xe^*+Xe^*\rightarrow Xe^++Xe+e$	8.0×10^{-11}	10
33	$He^{**}+Xe\rightarrow He+Xe^++e$	1.2×10^{-10}	16
34	$He^*+Xe\rightarrow He+Xe^++e$	1.2×10^{-10}	11
35	$He_2^*+Xe\rightarrow 2He+Xe^++e$	5.9×10^{-10}	16
36	$He^*+He^*\rightarrow He_2^++e$	1.5×10^{-9}	15
37	$He^*+He^*\rightarrow He+He^++e$	2.7×10^{-10}	22
38	$Ne+e\rightarrow Ne^++2e$	9.0×10^{-19}	12
39	$Ne^*+e\rightarrow Ne^++2e$	1.3×10^{-8}	12
40	$Ne^{**}+e\rightarrow Ne^++2e$	7.1×10^{-8}	12
41	$Ne_2^*+e\rightarrow Ne_2^++2e$	3.0×10^{-8}	12
42	$Ne_2^++e\rightarrow Ne^*+Ne$	$3.7\times10^{-8}\times T_e^{-0.43}$	20
43	$Ne_2^++e\rightarrow Ne^{**}+Ne$	$3.7\times10^{-8}\times T_e^{-0.43}$	12
44	$NeXe^++e\rightarrow Xe^*+Ne$	$2.0\times10^{-7}\times T_e^{-0.5}$	11
45	$NeXe^++e\rightarrow Xe^{**}+Ne$	$8.0\times10^{-8}\times T_e^{-0.5}$	20
46	$Ne^*+Xe\rightarrow Xe^++Ne+e$	7.5×10^{-11}	14
48	$Ne_2^*+Xe\rightarrow Xe^++2Ne+e$	1.0×10^{-10}	12
49	$Ne^*+Xe\rightarrow NeXe^++e$	1.8×10^{-11}	9
50	$Ne^*+Ar\rightarrow Ne+Ar^++e$	2.19×10^{-10}	21
51	$Ne^{**}+Ar\rightarrow Ne+Ar^++e$	5.50×10^{-10}	21
52	$Ne_2^*+Ar\rightarrow 2Ne+Ar^++e$	2.46×10^{-11}	21
53	$Ar+e\rightarrow Ar^++2e$	$1.75\times10^{-8}\times T_e^{0.68}\times e^{(-23.6/T_e)}$	10
54	$Ar^*+e\rightarrow Ar^++2e$	$5.18\times10^{-8}\times T_e^{0.67}\times e^{(-6.27/T_e)}$	10
55	$Ar^{**}+e\rightarrow Ar^++2e$	$1.41\times10^{-7}\times T_e^{0.61}\times e^{(-4.00/T_e)}$	10
56	$Ar^++2e\rightarrow Ar^{**}+e$	$7.2\times10^{-27}\times T_e^{-4.5}$	22
57	$Ar^++2e\rightarrow Ar^*+e$	1.0×10^{-19}	15
58	$Ar^++Ar+e\rightarrow Ar^*+Ar$	1.0×10^{-26}	15
59	$Ar_2^++e\rightarrow Ar^*+Ar$	7.0×10^{-7}	15
60	$Ar_2^++e\rightarrow Ar^{**}+Ar$	$1.5\times10^{-9}\times(T_g/T_e)^{0.43}$	10
61	$Ar^*+Ar^*\rightarrow Ar^++Ar+e$	5.0×10^{-10}	22
62	$Ar_2^*+Ar_2^*\rightarrow Ar_2^++Ar+e$	5.0×10^{-10}	10
63	$Ar^{**}+Xe\rightarrow Xe^++Ar+e$	2.0×10^{-10}	10

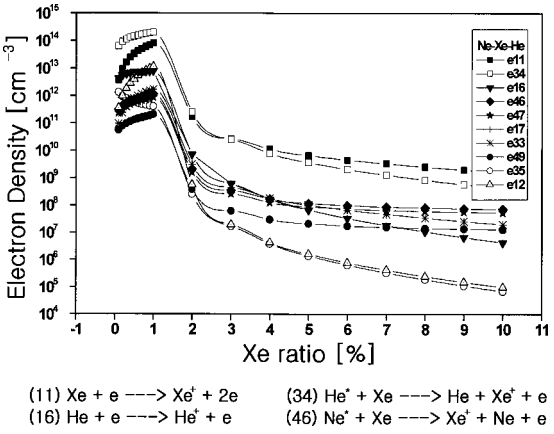

FIG. 7. Electron densities produced as a result of each reaction equation in a Ne–Xe–He gas mixture ($P=400$ Torr).

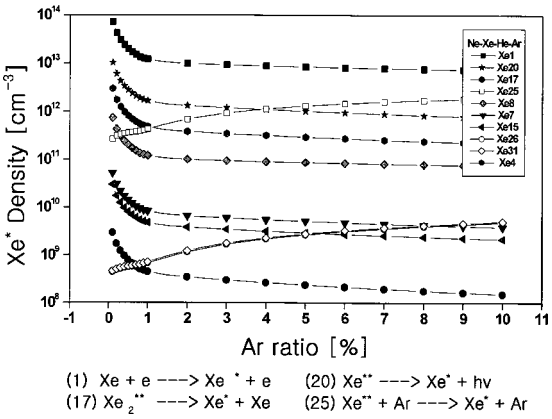

FIG. 9. Xe* densities produced as a result of each reaction equation in a Ne–Xe–He–Ar gas mixture (Xe=4%, $P=400$ Torr).

four-component gas He–Ne–Xe–Ar with Ar gas mixing ratio of around 0.5% will be lower than that of the three-component gas He–Ne–Xe.

Figures 5 and 6 show the Xe* densities that is produced and reduced, respectively, as a result of each reaction equation as a function of the Xe mixing ratio in the conventional He–Ne–Xe gas mixture. The equations inscribed below each figure are the dominant reactions. The number of the equation matches the number in the graph inset (The equations used in the chemical reaction simulation are summarized in Tables II and III.) As shown in Fig. 5, the proportion of the Xe* density produced by the direct excitation of Xe due to electron impact is at least above 85%. Thereafter, the second and the third largest proportions of Xe* are produced by $[Xe^{**}\rightarrow Xe+h\upsilon(828\,nm)]$ and $(Xe_2^{**}\rightarrow Xe^{*}+Xe)$, respectively. This explains that Xe* density is closely related to the electron density.

Figure 6 shows the decay mechanism of Xe* particles. Most Xe* particles are reduced through radiating 147 nm VUV$[Xe^{*}\rightarrow Xe+h\upsilon]$ or transforming into dimers (Xe_2^{*1}, Xe_2^{*3}). As the Xe concentration increases, the proportion of transforming into dimers radiating 152 and 173 nm also increases. Accordingly, the 147 nm radiation decreases whereas 152 and 173 nm radiation increase with an increase in the Xe concentration.

Figures 7 and 8 show the electron densities that are produced and reduced, respectively, as a result of each reaction equation with the He–Ne–Xe gas. Figure 7 shows that the dominant proportion of electrons is produced by the penning ionization between He and Xe when the Xe concentration is below 3%. However, with a Xe concentration above 3%, the dominant proportion becomes the electrons produced due to direct ionization. Figure 8 shows the decay mechanism. The reactions $[Xe_2^{+}+e\rightarrow Xe^{*}+Xe]$, $[Xe_2^{+}+e\rightarrow 2Xe]$, and $[NeXe^{+}+e\rightarrow Xe^{*}+Ne]$ are more dominant than any other reactions when the Xe concentration is below 1%. However, with a Xe concentration above 1%, electrons decayed by the recombination reaction between Xe_3^{+} and electron $[Xe_3^{+}+e\rightarrow Xe^{*}+2Xe]$ become the most dominant process. Most electrons are predominantly reduced by recombination with Xe_2^{+} or Xe_3^{+}.

Figures 9 and 10 show the Xe* densities that are produced and reduced, respectively, as a result of each reaction

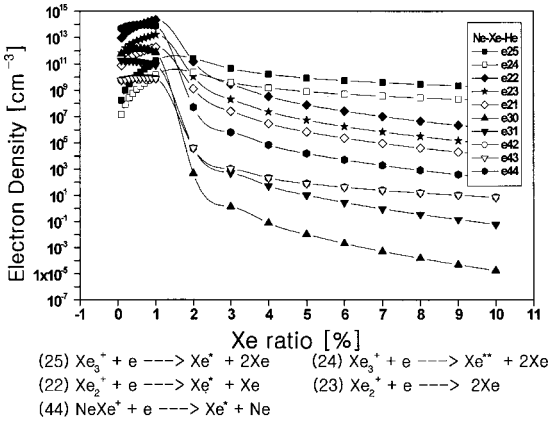

FIG. 8. Electron densities reduced as a result of each reaction equation in a Ne–Xe–He gas mixture ($P=400$ Torr).

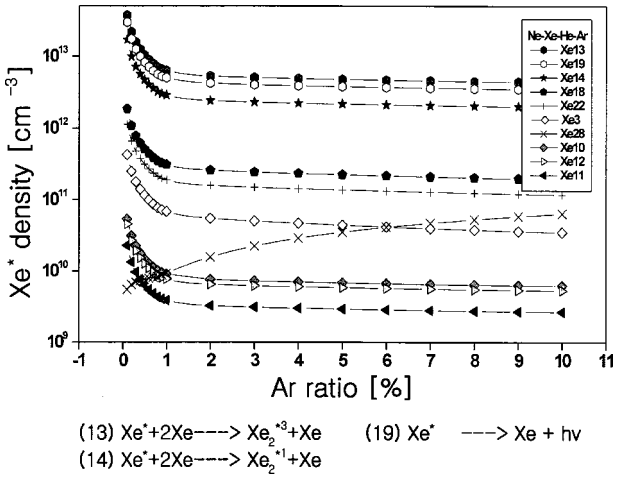

FIG. 10. Xe* densities reduced as a result of each reaction equation in a Ne–Xe–He–Ar gas mixture (Xe=4%, $P=400$ Torr).

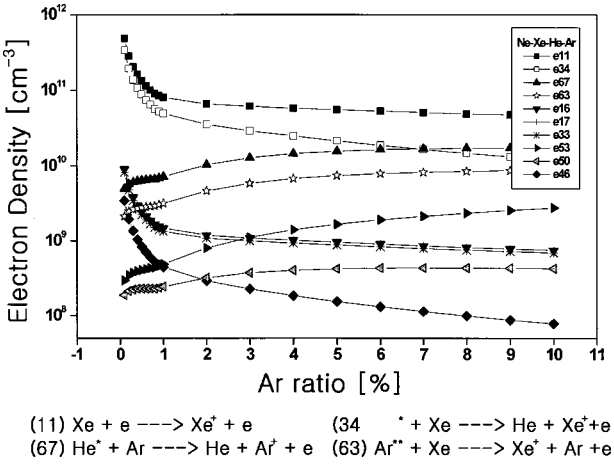

FIG. 11. Electron densities produced as a result of each reaction equation in a Ne–Xe–He–Ar gas mixture (Xe=4%, P=400 Torr).

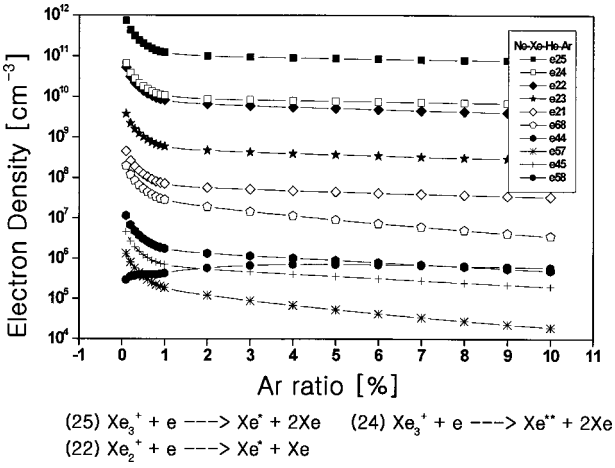

FIG. 12. Electron densities reduced as a result of each reaction equation in a Ne–Xe–He–Ar gas mixture (Xe=4%, P=400 Torr).

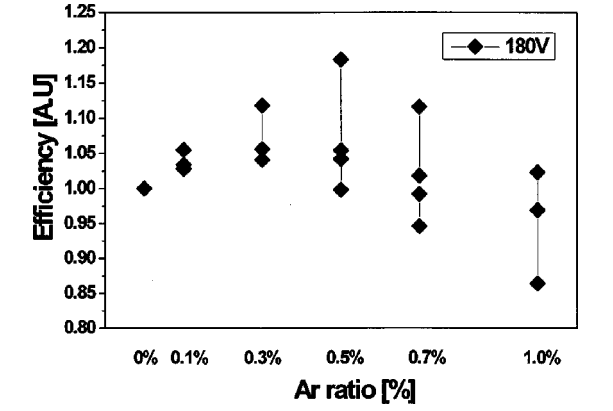

FIG. 13. Luminous efficiency as a function of Ar concentration in He–Ne–Xe(4%)–Ar.

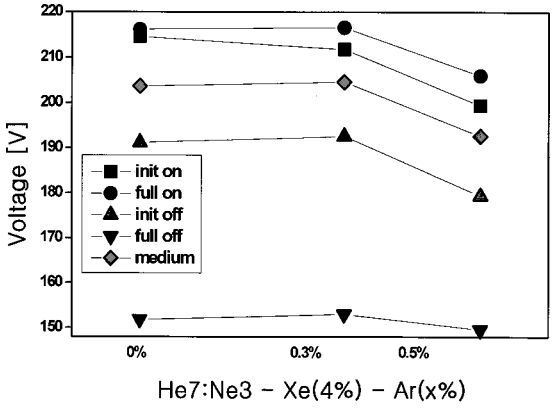

FIG. 14. Voltage characteristics at 400 Torr.

equation with the new combination He–Ne–Xe(4%)–Ar gas. Similar to the He–Ne–Xe mixture, the direct excitation of Xe is the most dominant in the production of Xe*. The Xe* density produced by [Xe**+Ar→Xe*+Ar] increases in proportion to the Ar mixing ratio. However, due to the decrease in the electron temperature, the total Xe* density decreases. Figure 10 shows that the Xe* decay mechanism in the four-component gas (He–Ne–Xe–Ar) is very similar to that in the three-component gas (He–Ne–Xe).

Figures 11 and 12 show the electron densities that are produced and reduced, respectively, as a result of each reaction with He–Ne–Xe–Ar gas. The dominant mechanism producing electrons in the four-component gas (He–Ne–Xe–Ar) is direct ionization. When a small amount of Ar is added, the electron temperature scarcely changes, however, numerous electrons are produced by [He*+Ar→He+Ar^{+} +e]. Yet, as the Ar ratio increase more, the electron temperature decreases and the total electron density decreases, as shown in Figs. 2 and 3. Figure 12 shows that the electron decay mechanism in the He–Ne–Xe–Ar gas is very similar to that in the He–Ne–Xe gas. As mentioned above, the addition of a small amount of Ar contributes to the production of electrons and Xe*, however, it does not play an important role in the decay mechanism. Accordingly, electron and Xe* densities are increased by adding a small amount of Ar.

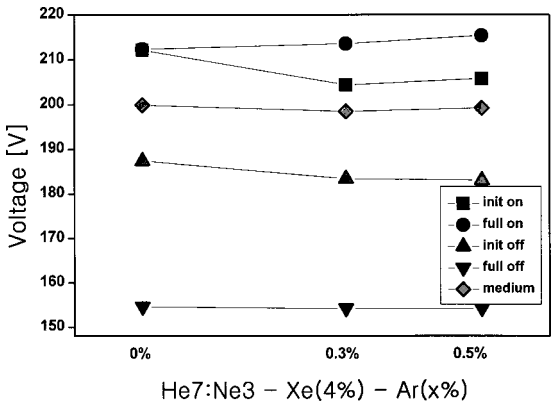

FIG. 15. Voltage characteristics at 500 Torr.

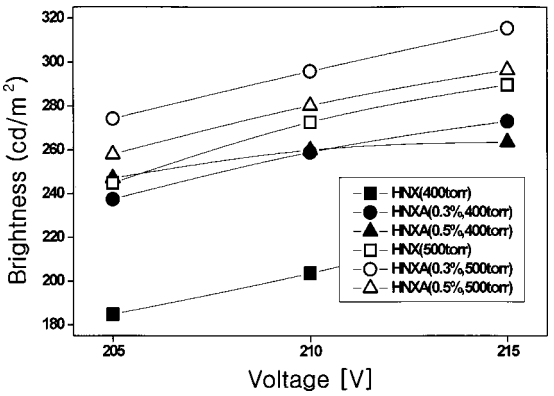

FIG. 16. Brightness vs voltage.

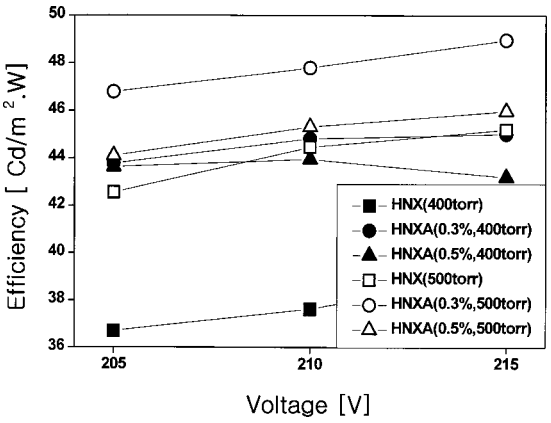

FIG. 18. Efficiency vs voltage.

Therefore nonlinear increase of electron density seemingly results from penning ionization caused by the Ar.

Figure 13 shows the luminous efficiency as a function of the Ar concentration. The experiment was performed in triplicate. Before each experiment, the panel was purified by heating (320 °C for 2 h) under vacuum condition. As shown in Fig. 13, the peak points appeared with 0.3% and 0.5% Ar concentrations. So, the voltage, brightness, power, and efficiency were all measured with Ar concentrations of 0%, 0.3%, and 0.5%.

Figures 14 and 15 show the voltages measured at 400 and 500 Torr, respectively. The medium voltage is the average of the full-on and initial-off voltages. When the pressure is 400 Torr, whereas the voltage characteristics are similar with 0% and 0.3% Ar concentrations, the voltages decrease with a 0.5% Ar concentration. On the other hand, when the pressure is 500 Torr, all voltages except for the full-on voltage are lower with 0.3% and 0.5% Ar concentrations than with 0% Ar concentration. In the above facts, the four component gas mixture including a small amount of Ar gas (He–Ne–Xe–Ar) has better characteristics on the driving voltage than three component gas mixture (He–Ne–Xe).

Figure 16 shows the brightness of each mixture gas. The brightness with a 0.3% Ar concentration is the highest among the three mixture conditions at the same pressure. The brightness increases by a maximum of 25%, compared with He(7):Ne(3)–Xe(4%) at 400 Torr. The brightness at 500 Torr is higher than that at 400 Torr. This indicates that the brightness increases as the pressure increases because more 173 nm is emitted than 147 nm as the pressure increases. Figure 17 shows the power consumption. As the Ar concentration and pressure increase, the power consumption also increases. Figure 18 shows the luminous efficiency of each gas mixture. Similar to the brightness, the luminous efficiency with a 0.3% Ar concentration is the highest. It increases by a maximum of 20% compared with He–Ne–Xe and the luminous efficiency at 500 Torr is higher than that at 400 Torr.

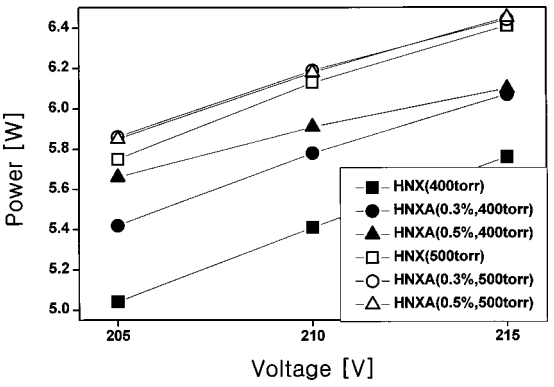

FIG. 17. Power consumption vs voltage.

IV. CONCLUSION

The electron, radical, and ion densities in the He–Ne–Xe–Ar discharge were investigated using a zero-dimensional simulation and the reaction mechanism was analyzed. The brightness and luminous efficiency were measured as functions of the pressure and mixing ratio. The simulation showed that the density of Xe*, directly related with 147 nm, has a peak value with an Ar mixing ratio between 0.1% and 0.5%. Furthermore, the luminance and luminous efficiency has a maximum value with an Ar gas mixing ratio of 0.3%. The results of the analysis of reaction mechanism indicate that the electron density is closely related to the Xe*($^1S_4$) density. When a small amount of Ar gas is added, the penning ionization between He and Ar produces large electrons responsible for the increase of the electron and Xe* densities.

In conclusion, when compared to the three-component gas He–Ne–4% Xe, the luminous efficiency in the four-component gas He–Ne–Xe–Ar is improved (about 20%) by the addition of 0.3% Ar gas due to the penning effect between Ar and He. Accordingly, He–Ne–Xe–Ar gas is proposed as a new high luminous efficiency gas for color PDPs.

ACKNOWLEDGMENT

This work was supported by the Development Program for the Examplary Schools in Information and Communication from the Ministry of Information and Communication (MIC).

[1]K. Takahashi and K. Tachibana, T. IEE Jpn. **111-A**, 182 (1991).
[2]S. Yoshikawa *et al.*, Japan Display' 92 Dig. 605 (1992).
[3]H. Uchiike, K. Miyake, and H. Shindo, Proc. SID **32/4**, 321 (1991).
[4]J. R. Wullert II *et al.*, Proc. SID **31/1**, 41 (1990).
[5]B.-K. Min, S.-H. Lee, and H.-G. Park, J. Vac. Sci. Technol. A **18**, 349 (2000).
[6]H.-G. Park, H.-Y. Choi, S.-H. Lee, J.-H. Seo, and K.-W. Whang, Trans. KIEE **47**, 372 (1998).
[7]K. C. Chio and K.-W. Whang, IEEE Trans. Plasma Sci. **23**, 399 (1995).
[8]D. J. Eckstrom, H. H. Nakano, D. C. Lorents, T. Rothem, J. A. Betts, M. E. Lainhart, D. A. Dakin, and T. E. Maenchen, J. Appl. Phys. **64**, 1679 (1988).
[9]M. Ohwa and M. Obara, J. Appl. Phys. **59**, 32 (1986).
[10]N. Nishida, T. Takashima, F. K. Tittel, F. Kannari, and M. Obara, J. Appl. Phys. **67**, 3932 (1990).
[11]H. Hokazono, K. Midorikawa, M. Obara, and T. Fujioka, J. Appl. Phys. **56**, 680 (1984).
[12]M. M. Turner and P. W. Smith, IEEE Trans. Plasma Sci. **19**, 350 (1991).
[13]M. Takei, K. Takahashi, Y. Murakami, T. Sakai, S. Hashiguchi, and K. Tachibana, ITEJ Tech. Rep. **14**, 55 (1990).
[14]M. Ohwa and M. Obara, J. Appl. Phys. **59**, 32 (1986).
[15]J. W. Wilson, R. J. Deyoung, and W. L. Harries, J. Appl. Phys. **50**, 1226 (1979).
[16]K. Takahashi, S. Hashiguchi, Y. Murakami, M. Takei, K. Itoh, K. Tachibana, and T. Sakai, Jpn. J. Appl. Phys., Part 1 **35**, 251 (1996).
[17]M. J. Kushner, J. Appl. Phys. **57**, 2486 (1985).
[18]S. A. Lawton, J. B. Richards, L. A. Newman, L. Specht, and T. A. DeTemple, J. Appl. Phys. **50**, 3888 (1979).
[19]M. Ohwa, T. J. Moratz, and M. J. Kushner, J. Appl. Phys. **66**, 5131 (1989).
[20]J. Meunier, Ph. Belenguer, and J. P. Boeuf, J. Appl. Phys. **78**, 731 (1995).
[21]O. Sahni, C. Lanza, and W. E. Howard, J. Appl. Phys. **49**, 2365 (1978).
[22]J. W. Shon and M. J. Kushner, J. Appl. Phys. **75**, 1883 (1994).